CellPress

Matter

Perspective

Leveraging cryogenic electron microscopy for advancing battery design

Diyi Cheng,[1] Bingyu Lu,[2] Ganesh Raghavendran,[2] Minghao Zhang,[2,*] and Ying Shirley Meng[1,2,*]

SUMMARY

The recent adoption of cryogenic electron microscopy (cryo-EM) in the battery field has boosted the understanding of electrochemically driven phenomena in batteries, particularly on metal anodes, metastable phases, and associated interfaces. With the advances in battery research by cryo-EM since 2017, concerns have arisen due to the differences in sample preparation and transfer procedures that could yield an inconsistent dataset and contradicting interpretations. Herein, we review the development of cryo-EM and its successful landings in different branches within the battery field, demonstrating how the knowledge gained by cryo-EM has advanced the understanding of battery systems. We emphasize that the discrepancies in this area will be eventually minimized when the optimized workflows are established for different materials. We further put forward our best practices for sample preparation during cryo-EM measurements with an outlook on artificial intelligence assisted data collection and analysis workflow that will benefit the entire material science community at large.

INTRODUCTION

Since the discovery of intercalation chemistry in the early 1970s,[1,2] battery technology has been rapidly developed through the efforts in expanding cathodes chemistry for higher energy density, exploring advanced electrolytes for nonflammability and wider voltage window, and enabling high theoretical capacity anode materials.[3] Research in the early era focused on the emerging chemistries of cathode materials that could deliver more capacity with good thermal stability and long cyclability, where TiS_2,[4] $LiCoO_2$,[5] and a vast variety of cathodes were invented based on the solid-solution concept (i.e., $LiMn_2O_4$,[6] $Li(Ni_xMn_yCo_z)O_2$,[7] $LiFePO_4$,[8] LNMO[9]). To resolve undesired nanoscale structural changes of cathodes that cannot be spatially resolved by X-ray- or neutron-based techniques, high-resolution imaging tools such as transmission electron microscopy (TEM) is crucially needed.[10]

In 1931, Ruska and Max Knoll[11] demonstrated the first TEM image on a platinum grid in Germany (Figure 1). Since then, TEM has been vastly applied throughout the material science field to identify crystal structures and diagnose material degradation at atomic scales. After decades of development, TEM continues to flourish in the battery field by demonstrating its power to determine the structural change and chemical composition evolution in cathode materials to pinpoint the battery degradation mechanism, such as the generation of defects and disordering phase in $LiCoO_2$ cathode after electrochemical cycling.[10]

After the tremendous research efforts into cathode materials and the advancing of electrolytes, the battery community realized that anode materials also deserve

Progress and potential

The initial invention of electron microscopy (EM) for high-resolution imaging of inorganic solids has been upgraded with the development of cryogenic functionalities in the recent decades, along with the continuous advances in imaging technologies (detectors, software), enabling the unequivocal identification of materials with high beam sensitivity. The adoption of cryogenic EM in the battery field has boosted the understanding of electrochemically driven phenomena in batteries, particularly on metal anodes, metastable phases, and associated interfaces. In this perspective, we give a brief overview of the development of cryogenic electron microscopy (cryo-EM) and review its success in different branches within the battery field, demonstrating how the knowledge gained by cryogenic EM has advanced the understanding of battery systems. We emphasize that optimized workflows are required for different types of materials to minimize the discrepancies in this field. We further put forward our best practices for sample preparation during cryo-EM measurements with an outlook on artificial intelligence assisted data collection and analysis workflow that will benefit the entire material science community.

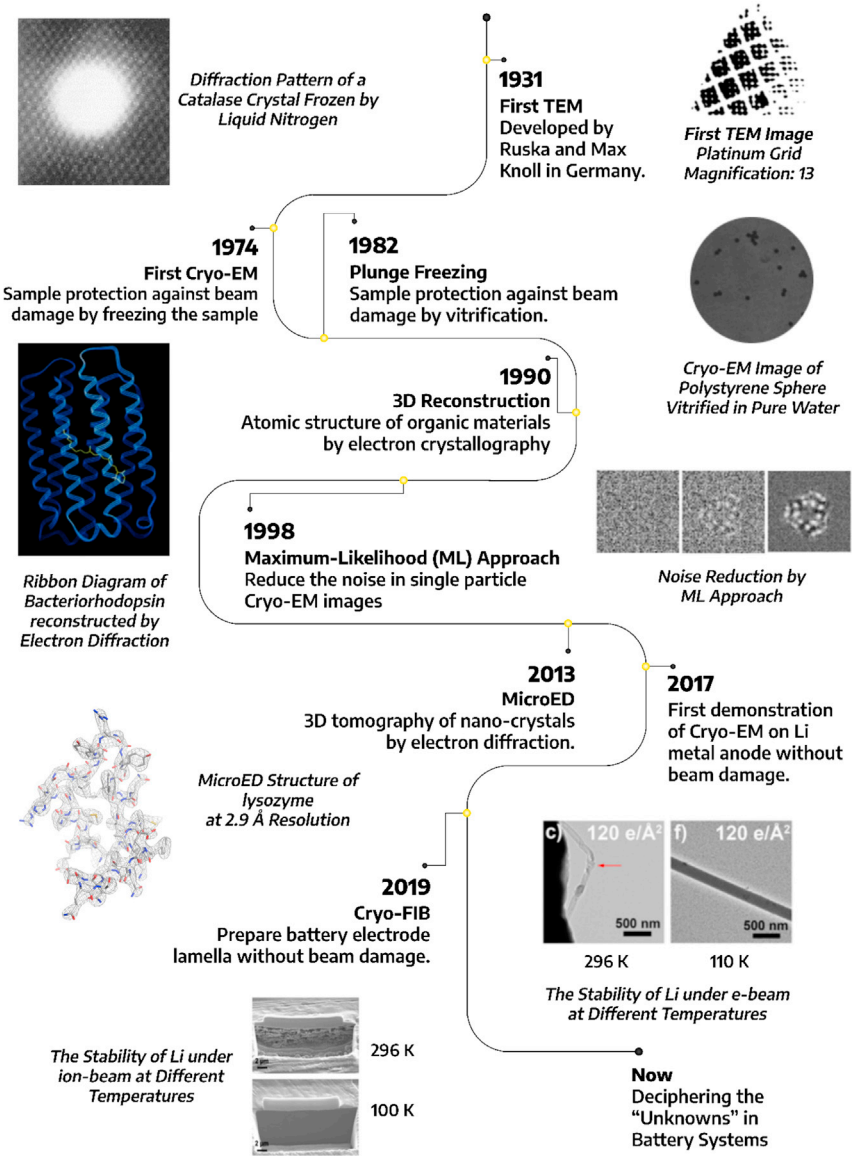

Figure 1. An overview
A brief history of cryo-EM development.

adequate attention for boosting the energy density of a battery, among which silicon and lithium metal anodes stand out as ideal candidates owing to their high theoretical capacities.[3] However, issues arose with the promises of these materials. Silicon anode follows an alloying mechanism upon lithium insertion into its structure, which causes a more than 300% volumetric expansion. The impact of such drastic physical change is profound; silicon anode structure easily collapses during repeated volume expansion and shrinkage; newly exposed fresh surface of silicon anode is prone to react with liquid electrolyte to form solid electrolyte interphase (SEI) that leads to the consumption of limited lithium source and an increased cell impedance upon cycling.[12] Differing from the case of Si, Li metal anode suffers from a dendritic metal growth during Li metal plating, where Li ions travel from cathodes and nucleate on the bare current collector or pre-existing Li metal surface. Due to the hardly controllable mass transfer in a mixed liquid system,[13] Li metal deposits tend to grow as

[1]Materials Science and Engineering Program, University of California, San Diego, La Jolla, CA 92121, USA

[2]Department of NanoEngineering, University of California, San Diego, La Jolla, CA 92121, USA

*Correspondence: miz016@eng.ucsd.edu (M.Z.), shmeng@ucsd.edu (Y.S.M.)

https://doi.org/10.1016/j.matt.2021.11.019

dendrites, which may penetrate through the polymer separator to cause short-circuiting of battery and raise safety concerns.[14]

In contrast, SEI is regarded as the most complex yet least understood components within a battery.[3,15] Presently, mysteries remain about the structures and chemical distribution of such interphases, hindering a further understanding of how they may impact battery performance.[16] In stark contrast with cathode materials, anode materials and associated interphases are generally more prone to the chemical and structural changes by electron beam irradiation due to joule heating and radiolysis,[17] while interphases might suffer additionally from electrostatic charging effects because of their insulating nature. To overcome the characterization barrier set by the beam intolerance and sizes, there has been a growing need to develop tools that can access nanoscale insights of beam-sensitive Li metal, Li alloy and their SEIs with minimized beam interference.

New functionalities were added on TEM in the structural biology field from 1970s. TEM was originally designed for imaging inorganic solids such as metal and oxides that have relatively high melting temperatures, strong chemical bonding, and resilience against high-energy electron beams. For imaging biological samples to identify their molecular structures, researchers in the structural biology field started to apply cryogenic protection for the beam-sensitive specimens. In early 1974, attempts to freeze the sample for protection under electron beam have enabled the collection of electron diffraction pattern of a catalase crystal after being frozen in liquid nitrogen[18] (Figure 1). Advances in cryogenic methodology quickly evolved to the adoption of a method named plunge freezing, during which the sample is frozen in amorphous ice by vitrification and can thus be protected. Such methods have enabled the TEM imaging of polystyrene spheres and are still extensively used in structural biology field.[19] The three decades following this development witnessed the rapid growth in structural biology field with the emergence of advanced characterization toolsets, including the three-dimensional (3D) reconstruction of organic material by electron crystallography,[20] noise reduction of TEM images via machine learning approach,[21] and 3D-tomography of nanocrystals[22] (Figure 1). Such developments have made imaging beam-sensitive biological materials and identifying their molecular structure at angstrom level a routine task, which amounts to the recognition by the 2017 Nobel Prize in Chemistry.

Concurrently, battery researchers realized that imaging anode materials can be potentially enabled by cryo-EM since anode materials are generally less susceptible to beam irradiation compared with biological samples. In 2017, two research groups in the United States adopted the sample preparation methodology and cryo-TEM instrumentation pioneered by the structural biology field, and successfully resolved the atomic structure of Li metal anode and its nanostructured SEI species.[17,23] Falling into the category of EM, another exemplary tool, namely, cryogenic-focused ion beam/scanning electron microscopy (cryo-FIB/SEM), has also been incorporated into battery field along with the introduction of cryo-TEM. This versatile tool provides large area examination of the beam-sensitive materials that complements the local information obtained by cryo-TEM[24] and offers cryogenic protection during TEM lamella preparation so that imaging beam-sensitive solid–solid interfaces becomes possible.[25] Such an interdisciplinary transition of characterization tools had a profound impact to the direction of battery field development. Since the first adoptions of cryo-TEM and cryo-FIB/SEM to characterizing the Li metal anode, there has been exponential growth in studies trying to implant cryogenic protection to investigate beam-sensitive material and interfaces within

battery system, ranging from alkaline metal anodes,[17,23,25–27] alloying anodes[28] to associated interfaces.[25,29]

In this perspective, we first look through the representative works applying cryo-EM in different branches of the battery research field, which has provided invaluable insights to advance the understanding of the battery system and enable better battery design. Then we propose several aspects pertaining to the concerns on the generation of different dataset and inconsistent data interpretation given the complexity of the tools, and how automation assisted by artificial intelligence can benefit the entire community with unequivocal data interpretation based on statistics.

CRYOGENIC PROTECTION FOR BEAM-SENSITIVE COMPONENTS IN BATTERY

Cryo-FIB/SEM characterization at bulk scale

Along with the adoption of cryo-TEM in the battery field, cryo-FIB/SEM has drawn much attention since its applications in both liquid and solid electrolyte (SE) systems (Figure 2A). As shown in Figure 2B, FIB/SEM uses high-energy ions such as gallium (Ga) ion to mill a certain amount of sample by designated patterns and depth, after which SEM is used to probe the freshly exposed surface or a lamella can be lifted out with the aids of a nanomanipulator.[24] However, due to the local heating and ion implantation during milling, beam-sensitive materials such as Li metal suffer from morphologic and chemical changes through the FIB process at room temperature.[24] To minimize such deleterious effects, cryogenic protection with the aid of liquid nitrogen is incorporated into FIB/SEM instrument to maintain sample at low temperature during operation, which has proven effective and critical for beam sensitive materials.

In detail, cryo-FIB/SEM works with a stage that is cooled down with nitrogen gas coming through a liquid nitrogen dewar (Figure 2B). Heat from the stage is constantly transferred to the carrier nitrogen gas so that stage temperature can be maintained around −180°C to −170°C. This process guarantees that the sample stays at a low temperature without the need for direct contact with liquid nitrogen, avoiding an undesired impact. In 2018, cryo-FIB/SEM was applied to examine the cross-sectional morphology of Li metal foil (Figure 2C). The cross-section of commercial Li metal foil after room temperature milling exhibits a porous structure with an adequate amount of Ga implantation, whereas the cryogenic temperature milling well maintains the fully dense feature of commercial Li metal foil without noticeable Ga ion implantation, demonstrating the necessity of applying a cryogenic temperature during FIB milling to preserve the pristine morphology and chemistry of beam-sensitive materials such as Li metal.[24]

Cryo-FIB/SEM further enables the 3D visualization of the material by coupling sequential milling/imaging steps and analysis software (Figure 2D). Such techniques have enabled the examination of Li metal deposit structure in three dimensions, quantitatively determining important parameters such as porosity, surface area, and components volume ratio that correlate with the performance of anode materials. Yang et al.[30] applied cryo-FIB/SEM to reconstruct the structure of Li metal deposited in different electrolytes, where the porosity and tortuosity of Li metal deposits were found to be positively related to the electrochemical performance of the specific liquid electrolyte (Figure 2E). Not limited to application in studying liquid electrolyte system, cryo-FIB/SEM has been confirmed effective for SE systems (Figure 2F). The 3D reconstruction of sulfide-based SE clearly unravels the internal

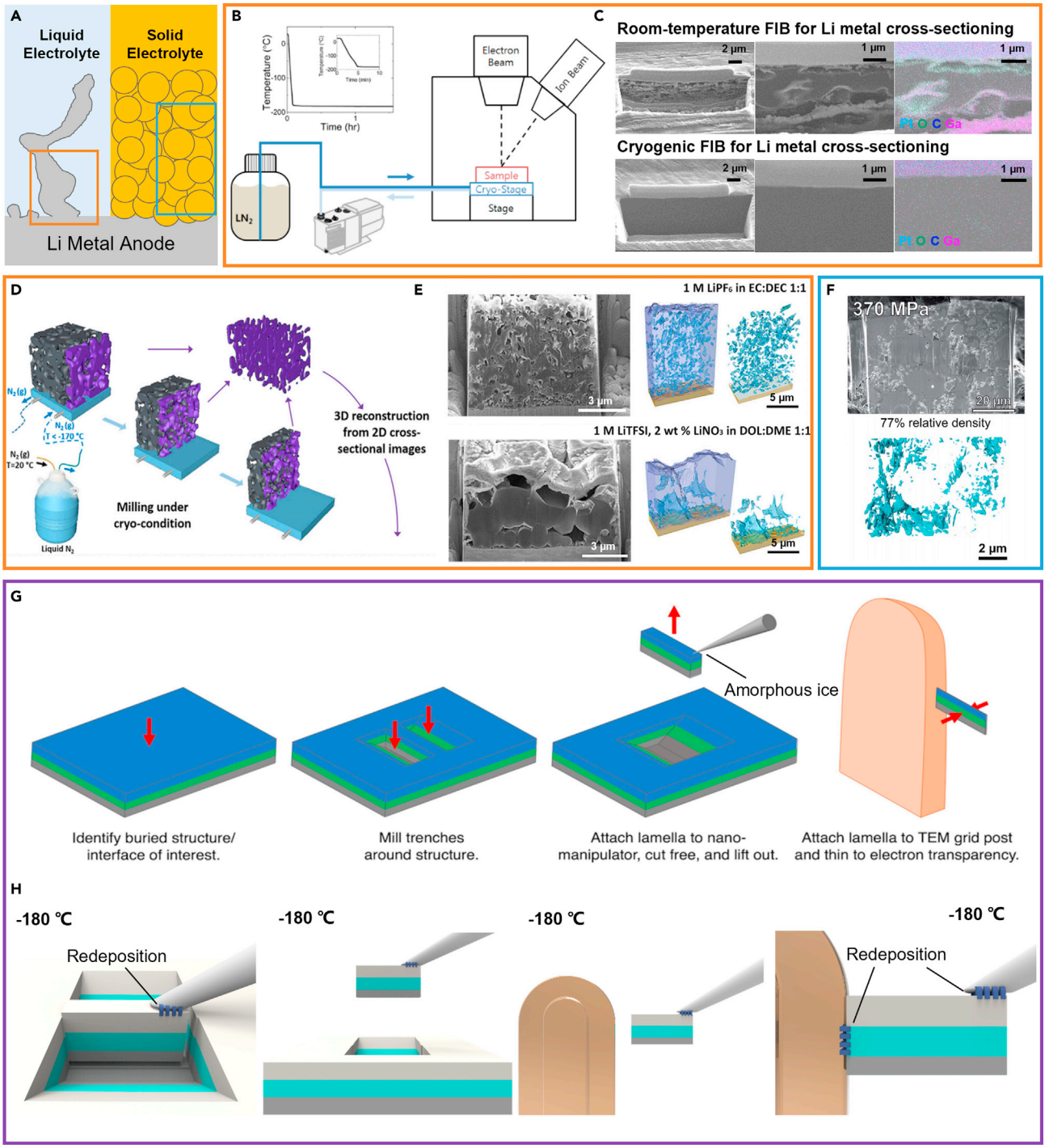

Figure 2. Cryogenic FIB/SEM for bulk and interface characterization

(A) Schematic showing Li deposits in liquid electrolyte and Li metal in contact with SE.

(B) Cryogenic FIB/SEM instrument configuration.

(C) Li metal cross-sectional morphology and chemistry difference by room temperature FIB and cryo FIB.

(D) Three-dimensional models demonstrating the workflow of 3D reconstruction.

(E) 3D reconstruction of Li metal in liquid electrolyte.

(F) 3D reconstruction of SE layer.

(G and H) Cryogenic TEM sample preparation methodology using amorphous ice (G) and redeposition material (H).

structure of a pressed SE layer, building a relationship between the applied stacking pressure and the porosity of SE.[31] Such buried interfaces or bulk materials have remained unclear before the application of cryo-FIB/SEM, which adds up the missing yet critical knowledge for better understanding how electrolytes affect anode operation and how morphology is correlated with electrochemical performance.

To date, conventional Ga ion FIB/SEM has been widely used for battery materials development, including interface/interphase characterization, 3D quantification, and simulation analysis. However, materials removal efficiency of the Ga ion FIB/SEM limits its capability to access representative area and volume in some battery materials systems, e.g., an electrode with tens of micron particle size. Recently, the emerging plasma FIB/SEM (PFIB/SEM) technology has been developed with different ion sources and high removal efficiency. It promises great potential for battery materials characterization by accessing representative two-dimensional area and 3D volume via a 40 times faster (than the Ga ion system) milling rate as well as enabling Ga-free sample preparation for alkali metal electrode through a nonreactive ion source (Xe^+ and Ar^+ ions).

Cryogenic FIB/SEM for TEM sample preparation

Due to the requirement of electron transparency, TEM samples are commonly prepared by FIB/SEM. Not limited to characterizing the bulk material from cross-sectioning and reconstruction, cryo-FIB/SEM gives a chance to beam sensitive materials for TEM examination. Differing from the room temperature TEM sample preparation process in FIB, the common material, organometallic platinum, as the connection media between a lamella and a nanomanipulator cannot be well-controlled or -patterned at a cryogenic temperature. To lift out the lamella from bulk sample at cryogenic condition then becomes an important step to bridge cryo-FIB/SEM preparation and cryo-TEM measurement.

There are two generally accepted methodologies for cryogenic liftout (cryo-liftout), as shown in Figures 2G and 2H. After the lamella is trenched from the bulk sample, a temperature-controlled nanomanipulator needle is inserted and made contact with the top edge of the lamella. A gas injection system then releases water vapor to designated patterns and region to form amorphous ice so that the lamella and the needle can be connected, after which the lamella is lifted out from the bulk sample and mounted on TEM grid applying the same method, ready for final cleaning and thinning.[25]

Another liftout method uses the redeposition mechanism during the FIB milling process. When the sample is bombarded by incoming Ga ions, surface materials are sputtered away in the forms of atoms, ions, and clusters from their original positions and flying around in a vacuum.

Depending on the ion beam intensity and sample geometry, a certain amount of sputtered materials would redeposit on nearby surfaces in an amorphous form. When applying redeposition for cryo liftout, the nanomanipulator is parked at the top edge of the lamella, where a series of parallel cross-section milling patterns are used to mill the material from lamella so that it redeposits around the pattern region and fills the gap. Then, the manipulator can be connected with the lamella (Figure 2H) by the redeposited material. After extracting the lamella from the bulk material, it is mounted on a TEM grid using the same protocol.[29]

Amorphous ice is convenient and easier to apply as a connection material; however, there is a large chance that the reactive material itself such as Li metal can react with water vapor during the liftout process and lead to undesired surface chemical

changes. To the contrary, the redeposition method avoids the use of water vapor and uses the material itself for connection, which minimizes the impact of sample reactivity. Nevertheless, the redeposition method requires experience and careful examination before it can be applied on the sample, giving rise to a larger chance of failure during cryo liftout. Even so, both methods are compatible with TEM sample preparation that particularly needs cryogenic protection, which bridge cryo-FIB/SEM and cryo-TEM so that a bulk-to-nanoscale characterization on beam-sensitive material becomes possible.

ADVANCING THE UNDERSTANDING OF BEAM-SENSITIVE ELECTRODES AND ASSOCIATED INTERFACES

SEI and inactive components identification in metal anodes

In 2017, two groups first explored the possibility of applying cryo-EM to study Li metal and associated interphases. Li et al.[23] demonstrated the atomic structure of Li metal that was electrochemically deposited on a copper mesh TEM grid[23] (Figure 3A). Two distinct SEI structures are identified, a multilayered and a mosaic structure, both with nanocrystalline inorganic species embedded in an organic amorphous matrix, consistent with the long-existing SEI models proposed in the 1980s and 1990s[32,33] (Figure 3B). Wang et al.[17] observed the nanostructure of electrochemically deposited Li metal under cryo-EM and identified the existence of lithium fluoride (LiF), a SEI component that has been proposed as one of the most important species. Since the first introduction of cryo-EM to the battery field, Li metal research rapidly rejuvenated owing to this new suitable tool that can access nanoscale insights on metastable phenomena of beam-sensitive components, enhancing the existing knowledge of electrochemically deposited Li metal and associated SEI species while also challenging conventional perspectives on SEIs.

One of the famous debates that pertains to the dominating effects of SEI on Li metal anode cycling performance is on the role of LiF, which is predicted to form and dominate in the SEI when a fluorinated electrolyte is used.[34] LiF is regarded as a species that facilitates the Li metal deposition due to its high stability against Li metal and low electronic conductivity; however, the low ionic conductivity of LiF cast doubts on whether this species can improve the transport and kinetics at the interphase during battery operation.[29] Further examination of SEI species on electrochemically deposited Li metal shows the evidence of crystalline LiF in SEI[35] (Figure 3C). Later Cao et al.[36] used a fluorinated orthoformate-based electrolyte for Li metal deposition, where a fully amorphous monolithic SEI on the order of 10 nm is identified on the surface of deposited Li metal. Fluorine signal within such an amorphous layer is detected via energy dispersive spectroscopy spectra (EDS).[36] The improved electrochemical performance is claimed to be the result of the formation of such fluorine-containing amorphous SEI. However, dissent was proposed soon by Huang et al.,[27] who observed that LiF exists in a form of nanoparticle covered by lithium oxide (Li_2O) and distributes near the bottom vicinity of Li metal dendrites. Elemental mapping by scanning TEM/electron energy loss spectroscopy (STEM/EELS) shows the absence of fluorine signal on the surface of Li dendrite,[27] further questioning the role of LiF for stabilizing SEI.

Besides the investigation on LiF, the existence and role of lithium hydride (LiH) species has also raised considerable debates in the field. LiH was first identified by Zachman et al.,[25] who successfully preserved cycled Li metal anode with liquid electrolyte as a whole entity in its original configuration by freezing the coin cell and transferring to cryo-FIB/SEM. Adopting 3D reconstruction in cryo-FIB/SEM and

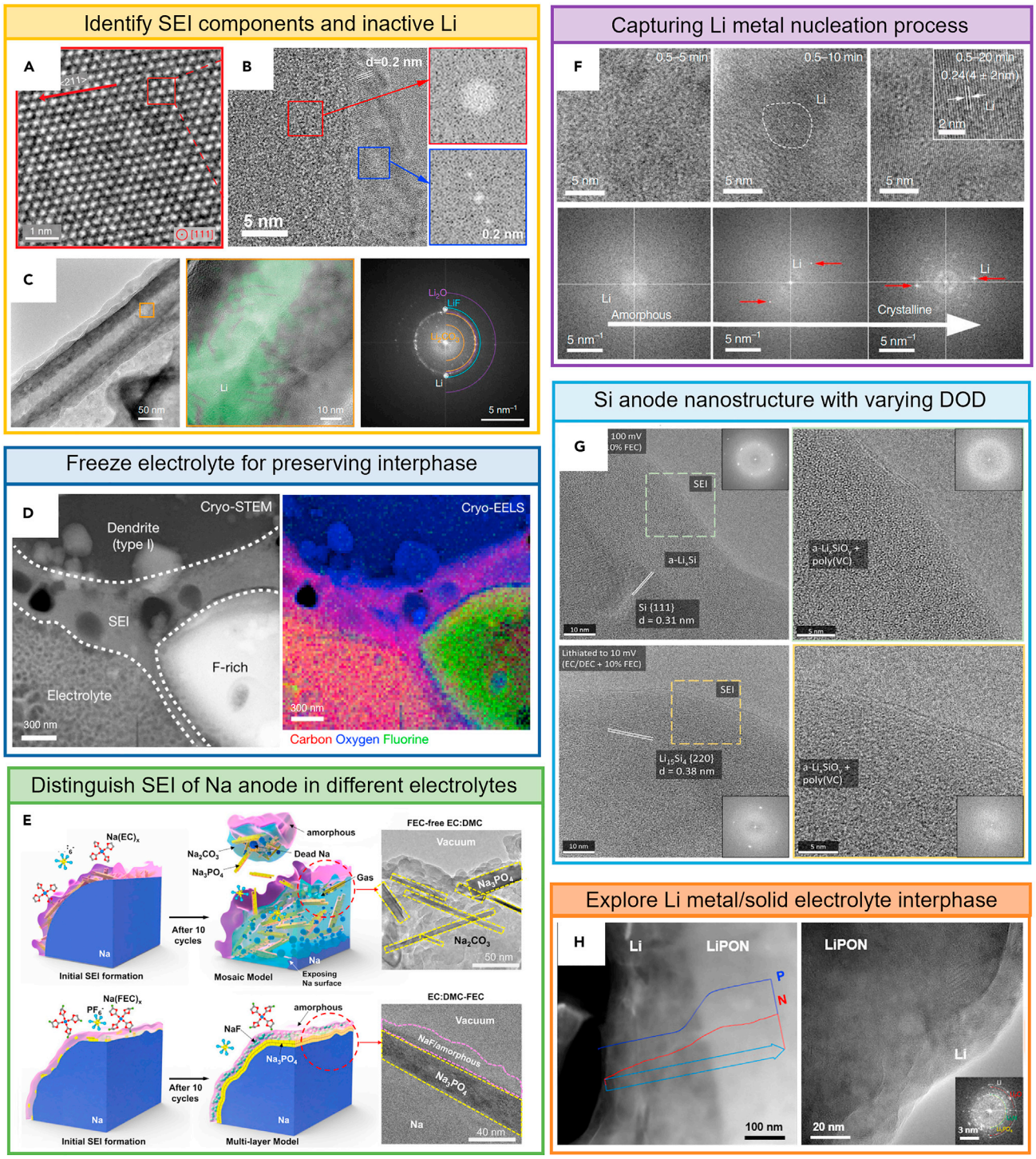

Figure 3. Nanoscale characterization by cryo-EM

(A–C) Cryo-EM for identifying (A) Li metal nanostructure, (B) the SEI component, and (C) inactive lithium distribution within Li dendrites.

(D) Cryo-STEM imaging and EELS elemental mapping of Li metal within frozen electrolyte.

(E) SEI components of Na metal anode in different electrolytes.

(F) Li metal nucleation process captured by cryo-EM.

(G) Si anode nanostructure at varying depth of discharge (DOD).

(H) Li/LiPON interphase uncovered by cryo-STEM image, cryo-STEM-EDS linescan and cryo-TEM.

cryo-STEM/EELS, an extended SEI layer wrapping around Li metal dendrites is found, with a majority of oxygen signal detected (Figure 3D). Two types of Li dendrites with distinct sizes and morphologies are unraveled, where LiH is identified by EELS for the first time in Li dendrites. Nevertheless, another work from Fang et al.[35] excluded the presence of LiH in either SEI or bulk Li deposits using titration gas chromatography (TGC) and residual gas analyzer. The dispute regarding the existence of LiH also raised concerns on the LiF detection through TEM measurements by earlier literature since there is a chance that LiF and LiH species are mislabeled due to their similar lattice spacings.[37] Attempting to address the argument, Shadike et al.[37] applied synchrotron-based X-ray diffraction and claimed both LiH and LiF species exist in SEIs. Although more evidence is needed to have a solid conclusion on the presence of LiH and its impact on anode performance, LiH is proposed to form solid solutions with LiF and facilitate Li transport through interphases.[37] Such controversy has inspired increased research efforts on SEI, while prompting the battery community to look for ways to regulate cryo-EM data collection and interpretation by establishing standardized protocols to resolve the long-debating issues such as the role of LiF and LiH.

Another factor that closely correlates with the cycling performance of Li metal anodes is the formation of inactive lithium during cycling. Nonuniform SEI and Li deposits are produced due to the inhomogeneous Li metal nucleation and growth. Inactive lithium generates when nonuniform Li deposition and dissolution lead to the cleavage of thin Li deposits and electronically insulating SEI layers.[38,39] The loss of the electron pathway renders the Li metal wrapped within SEI unable to be dissolved as Li ions and make this portion of Li metal inactive, resulting in the degradation of Li metal anodes. Cryo-EM also turns out to be a powerful tool to identify how the inactive lithium is distributed within Li deposits and how inactive lithium formation correlates with the performance of Li metal anode when coupled with TGC, further improving the understanding of the failure mechanism of Li metal anodes[35] (Figure 3C). Knowledge gained from cryo-FIB/SEM and cryo-EM examinations have shifted the focus of Li metal research from eliminating Li dendrite growth to suppressing the formation of inactive lithium on the Li metal anode during battery operation.

Apart from Li metal batteries, new insights gained via cryo-EM also benefit other alkaline metal batteries, among which sodium (Na) batteries are now regarded as a promising technology particularly applicable in grid storage owing to the low cost of the Na element and its abundance in the earth's crust. To enable the use of Na metal, a deep understanding of SEI formation on Na anodes is gained via exploring the effects of fluorinated ethylene carbonate (FEC) on the cycling behavior of Na metal anode. It is found that Na metal surface forms a multiplayer SEI structure containing sodium fluoride (NaF) and sodium phosphate (Na_3PO_4) when FEC is added into the electrolyte, exhibiting a greater stability compared with the SEI formed without FEC additive[40] (Figure 3E). To practically use the high theoretical capacity of metal anodes, new strategies to minimize SEI growth and regulate metal deposition await new insights to be unveiled by a wider adoption of cryo-EM, which is a trend for the future.

Probing nucleation behavior of metal anodes

To resolve the nonuniform metal deposition that leads to the formation of dendritic metal growth and subsequent inactive components, a comprehensive understanding of metal nucleation process in the early stage is critically needed. Wang et al.[41] applied cryo-TEM to look at the Li metal nucleation process, where an

amorphous-to-crystalline transition that can be tuned by current density and types of liquid electrolytes was observed (Figure 3F). Insights gained from such glassy metal formation at an early stage during Li metal deposition not only gives rise to new strategies on minimizing nonuniform Li metal plating, but extends the nucleation study on other metal species, i.e., Na, K, Mg, and Zn. The similar glass formation discovered for these metals during deposition are distinct from common fast quenching process, calling for attention on electrochemically driven formation of metallic glasses that can be used for various applications. An alternative solution to regulate Li metal nucleation is the use of seeding layers that commonly include lithophilic metal species (i.e., Au, Ag) and metal compounds (i.e., MoS_2). Work performed by Tao et al.[42,43] demonstrated the advantage of offering nucleation sites for Li metal deposition that results in homogeneous growth of nondendritic Li deposits.

Ideally, Li metal ought to nucleate uniformly on the surface of the current collector and grow homogeneously to form large granular Li deposits with a columnar structure. In the very beginning of Li metal nucleation, factors such as current densities, electrolytes, or seeding layers could play an important role. However, on a microscale level, external parameter control turns out to be crucial in determining the nucleation behavior of Li metal. Deploying cryo-FIB/SEM to observe the Li deposition morphology in the presence of different uniaxial pressures during battery cycling, Fang et al.[44] show that a columnar Li deposit structure with large grain sizes is achieved when the cell runs under a pressure of 350 kPa, where Li metal tends to form more homogeneous nucleates and evolves to a dense, low tortuosity, and uniform deposit layer regardless of current densities or electrolyte types. A Li metal reservoir with such characteristics is consequently important for uniform Li metal deposition.[44] This work puts forward a universal strategy that can potentially boost the cyclability of Li metal anode in practical use by tuning the morphology of Li deposits to reduce SEI formation and inactive Li accumulation, which also provides a guideline and potential solutions for other metal anode deposition processes.

Progress in other anode systems

The ubiquity of cryo-EM as a powerful analytic tool is not monopolized by the metal anode field. Graphite material has long been adopted in commercialized products owing to its stability and modest capacity.[3] It is well-known that graphite is incompatible with propylene carbonate (PC) electrolyte due to the exfoliation effects upon lithiation. Recently Han et al.[45] found that graphite exfoliation occurs even with an ethylene carbonate (EC)-based electrolyte, a compatible analogue instead of PC, when an aggressive formation process is applied. Detailed analysis gained by cryo-EM sheds light on the importance of electrolyte additives such as vinylene carbonate and provides a mechanistic understanding of the impact of proper formation protocol on graphite anodes.[45]

Promising for its high theoretical capacity, Si anode suffers from poor cyclability due to the drastic volumetric changes during lithiation and delithiation. An electrolyte additive FEC has been used for improving the cyclability while the underlying root cause remains elusive. Huang et al.[28] deployed cryo-EM on Si anodes at different lithiation/delithiation states, where the SEI consisting of poly vinylene carbonate is found to be stable against oxidation and remains conformal after delithiation, contributing an enhanced cyclability (Figure 3G). Recently, He et al.[46] further unveiled the correlation between the structural and chemical evolution of Si and its SEI in three dimensions by integrating EDS tomography, cryo-STEM, and an advanced algorithm, where SEI is shown to grow toward the interior of the Si

electrode and form dead Si as a consequence of continuous void generation during the repeated delithiation processes.

An overview of anode study by cryo-EM emphasizes the importance for establishing appropriate protocols to protect beam sensitive anode materials during characterizations, featuring the vital role of cryo-EM on obtaining mechanistic understanding of complex metastable phenomena within anode materials.

New insights in cathode and associated interphases

Moving forward to the counter electrode in the battery system, cathode materials are generally more resilient under an electron beam compared with anodes. Although cathodes have been intensively studied at an atomic scale in the past few decades by normal EM, with the ascending attention for interphase-controlled performance, cathode electrolyte interphase (CEI) also awaits rigorous research efforts. Due to the highly oxidative environment on the cathode surface during the charging process, most electrolytes decompose and form a thin layered material covering on the cathode. To access such a thin layer that is also air- and beam-sensitive, cryo-EM finds a way to explore the properties of CEI.

Alvarado et al.[47] studied the impact of sulfone-based liquid electrolyte on the performance of high-voltage LNMO cathode using cryo-EM, where the CEI found in baseline electrolyte exhibits a nonuniform coverage on LNMO surface, increasing the chance of cathode surface being exposed to fresh electrolyte and consuming Li source. However, the CEI found in the advanced electrolyte demonstrates a conformal coverage on LNMO particles with an evenly distributed thickness around 0.612 nm, well-correlated with the improved electrochemical performance.[47] An analogous reduced CEI thickness and uniform CEI coverage on $LiNi_{0.6}Mn_{0.2}Co_{0.2}O_2$ (NMC) cathode have also been identified by Yang et al.[48] when coupled with a liquid gas electrolyte system. In another study by Zhang et al.,[49] the NMC cathode particle forms a uniform CEI layer after an electrical shorting treatment at pristine state, leading to an improved capacity retention and reduced cell impedance.

Apart from solely demonstrating the morphology of CEI layers, cryo-EM also helps to identify the CEI species for sulfurized polyacrylonitrile (SPAN) cathode. In an ether-based liquid electrolyte system with a lithium nitrate ($LiNO_3$) additive, the CEI formed on SPAN particle consists of LiF and lithium nitrite ($LiNO_2$), believed to be the key for the enhanced cyclability of a SPAN cathode.[50]

New insights on cathode study by cryo-EM have drawn more attention to the interphase-pivoted electrochemical performance. Nevertheless, compared with anode systems, the uniqueness of cryogenic protection for cycled cathodes has not been well-acknowledged in the literature. Detailed imaging parameter control such as electron dose needs to be well-documented depending on the types of cathodes and state of charges, because highly charged cathodes exhibit a much higher beam sensitivity and chemical reactivity. Without proper protection, the electron beam especially under scanning mode can induce phase transformation of the cycled cathode materials more than the electrochemical cycling itself.

Accessing buried solid–solid interfaces

Unlike a solid–liquid interface, which is more convenient to access, solid–solid interfaces in batteries are generally difficult to characterize due to their buried nature and equally high reactivity to ambient and beam irradiation. In the case of all solid-state battery, a complex interface commonly forms between Li metal and SEs due to

chemical or electrochemical incompatibility. Among common SEs, oxides are generally more beam tolerant, which enables high-resolution STEM imaging of their crystal structures and interphases with metal anode.[51–54] In contrast, other SEs made of sulfides, halides, nitrides, and polymers are prone to beam damage due to their intrinsic properties such as low electronic conductivity or weak chemical bonding. The formation of electrically insulating species upon decomposition between SEs and Li metal adds on difficulties for probing such solid–solid interfaces. Cryogenic protection turns out to be a solution for probing some of the SEs.

By combining cryo-FIB/SEM and cryo-(S)TEM, Cheng et al.[29] preserved and observed the pristine interface between Li metal and a well-known SE, lithium phosphorus oxynitride (LiPON) (Figure 3H). This interface is found to be 80-nm thick with Li_2O, Li_3N and Li_3PO_4 embedded in an amorphous matrix. Such an ionically conductive and electronically insulating thin interphase is proposed to be key for the stable nature between Li metal and LiPON.[29] Besides the Li/LiPON system, the solid–solid interface between Li metal and a polymer SE, poly(ethylene oxide) (PEO) has also been investigated by cryo-EM. Sheng et al.[55] unveil a Li/PEO interface comprising nanocrystalline Li_2O, LiOH, and Li_2CO_3 species that are incorporated inside an amorphous phase. The polycrystalline features of Li metal in the vicinity of PEO indicates the drastic thermodynamic instability that could lead to side reactions and increased cell impedance. A mitigation strategy is then proposed by adding Li_2S to prevent the continuous reaction between Li metal and PEO. By coupling cryo-EM, XPS, and computational methods, Li_2S is shown to accelerate the decomposition of $LiN(CF_3SO_2)_2$ (LiTFSI) that gives rise to an LiF-rich interphase between Li metal and PEO that stabilizes the polymer electrolyte and enhances the ion transport properties.[55]

Cryogenic protection proves effective in preserving the structure of beam sensitive SE materials, whereas conducting high-resolution TEM (HRTEM) imaging on sulfide-based SE turns out to be extremely difficult. One of the main reasons is that the irradiation damaging mechanism for sulfide is considered as electrostatic charging effect, where cryogenic protection does not apply. Investigating sulfide material will then require reducing the size of TEM sample to shorten the electron conduction pathways, in combination with advanced imaging techniques (i.e., ultralow dose [S] TEM) and other protection methods such as electronically conductive coatings.

FUTURE OUTLOOK FOR CRYO-EM WORKFLOW AND DATA INTERPRETATION

The introduction of cryo-EM technologies in the different branches of battery research undoubtedly revived the efforts of achieving a practical metal anode battery with better cathodes for higher energy density and prolonged cyclability. Although the application of cryo-EM in batteries seems promising, herein we list out several concerns pertaining to the regulation of cryo-EM study that calls for attention: (1) the limitation of cryogenic protection, (2) cryogenic sample transfer protocols, (3) consistent data collection and reliable data analysis, and (4) the dearth of knowledge for phase change of complex materials at low temperature.

Cryogenic protection is applied on material to avoid damage on its structure or chemistry from electron beam irradiation. The damage mechanisms fall into two main categories, namely, elastic scattering (electron–nucleus interaction) and inelastic scattering (electron–electron interaction)[56] (Figure 4A). When elastic scattering damage occurs, accelerated electrons with high kinetic energy reaching the

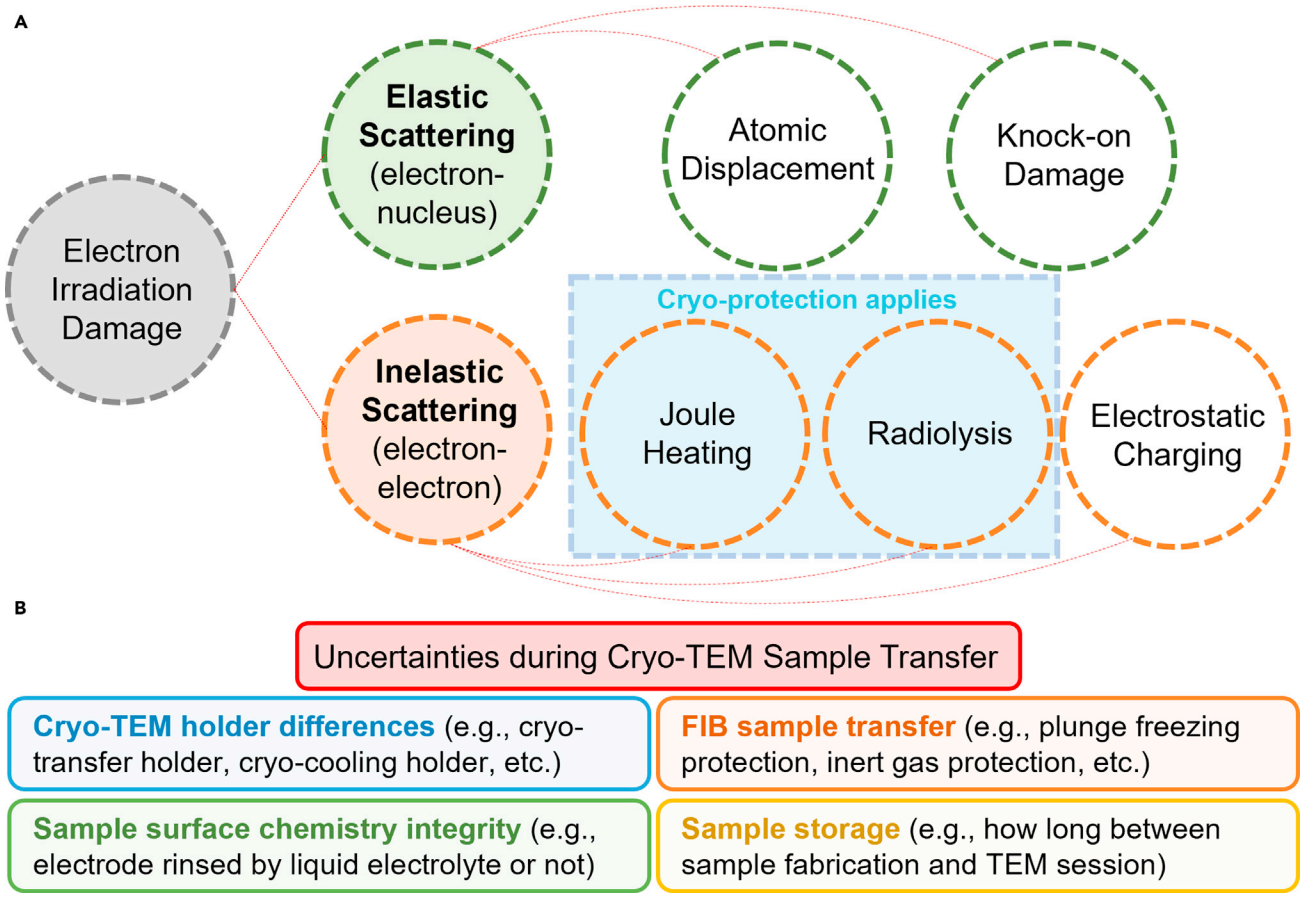

Figure 4. Potential concerns during cryo-EM examination

(A) Schematic of electron irradiation damage mechanisms, where only beam damage from Joule heating and radiolysis can be mitigated by cryogenic protection.

(B) Uncertainties during cryo-TEM sample transfer that can lead to inconsistent data collection and interpretation.

specimen surface lead to the displacement of atoms within the specimen. Atoms are knocked off when the momentum transferred from electrons is high enough, resulting in irradiation damage. Alternatively, inelastic scattering damage occurs due to the interaction between incoming electrons and specimen electrons, which may cause overly joule heating, radiolysis, and electrostatic charging.[57] Note that, of all the damage mechanisms, only joule heating and radiolysis can be mitigated by cryogenic protection, stressing the importance of knowing the damage mechanisms of target material before choosing the right way for protection from irradiation.

The complexity of cryo-EM characterization determines that the discrepancies can be easily generated during the many steps of operation or generated as a result of diverse sample handling protocols. Such uncertainties lie in the whole sample transfer procedure, where cryo-TEM holder choices, cryo-FIB sample transfer process, metal anode sample washing process, and TEM sample storage before actual TEM sessions all need to be regulated with standardized protocols or well-documented in the publication (Figure 4B). Specifically, TEM holder choices between cryo-transfer holder and cryo-cooling holder could lead to data discrepancies due to the various amount of air exposure during the transfer[58]; cryo-FIB sample transferred through plunge freezing protection suffers from icing problem; metal anode TEM samples should not be washed by liquid electrolyte to maintain the surface

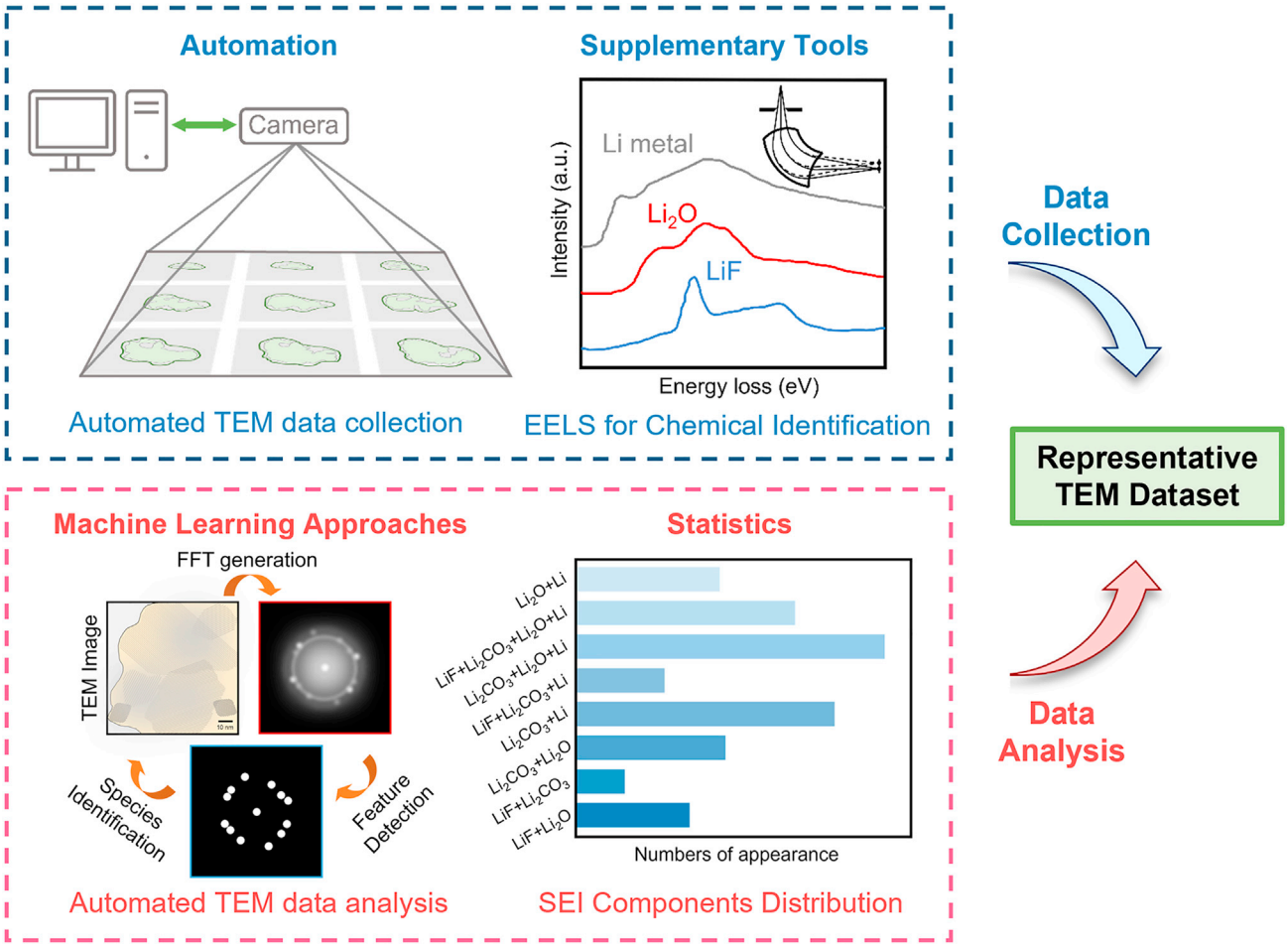

Figure 5. Workflow of an AI-assisted TEM data collection and analysis

chemistry integrity; the storage time for the TEM sample before actual measurement is also likely to cause result discrepancies even in the atmosphere-controlled glovebox. All uncertainties above need to be handled before trustworthy data can be generated.

Another solution to ensure a consistent dataset is the implantation of artificial intelligence (AI) technology into the EM examination process, during both data collection and data analysis (Figure 5). Automated TEM image acquisition will benefit from large batch data acquisition and reduce the human errors caused by potential beam alignment issues, incorrect target material locating, or inconsistent image acquisition parameters.[59] TEM images must be coupled with techniques such as EELS to confirm the characteristic chemical signature of target species.[60] Once a dataset is collected, the analytic process requires new approaches that are capable of handling datasets of gigantic size with high efficiency and accuracy, with AI being a potential solution. Recently, there has been a renaissance in AI-assisted data post-processing, owing to the success of deep learning (DL).[61–63] However, certain limitations present in these studies due to the use of datasets from one specific sample[62] and the lack of a universal model for all the high-resolution images from one dataset. Thus, it is essential to develop coding tools that can be equipped with DL to process multiple TEM images and use suitable segmentation method to extract features

such as the spots in fast Fourier transform (FFT) patterns so that crystallographic information about the specimens can be processed and summarized in an accurate way. The subsequent outputs eventually yield conclusions that can be based on statistics. Meanwhile, the emergence of automated analysis methods in materials science calls for adequate computational capability, which has given rise to open-source software and web-based hosting services.[64,65] Nevertheless, such analytical tools require an appropriate computational environment with necessary storage for operation. To avoid constantly upgrading and setting up the limited local computational environment (i.e., personal computers), cloud computing helps to achieve high-throughput data analysis using a software-as-a-service (SaaS) model, although data privacy and security remain an issue.[66,67] Hence, the development of web platforms that can provide material simulation and analysis, and supercomputer facility that allows real-time access for such TEM data processing will be imperative for the success of automated big data analysis.

The deployment of cryo-EM into the battery field in the past 4 years has motivated many more efforts in studying the beam-sensitive interfaces and other crucial components lying at nanoscale, and provided invaluable insights for advancing battery design. The research focus of Li metal anode has shifted from suppressing dendrite growth to eliminating inactive lithium accumulation. Newly gained knowledge enabled morphology-controlled uniform Li metal deposition that can be tuned by nucleation process, interface engineering, and external uniaxial pressure. Cryo-EM applications in other branches of battery research have shed light on the correlation between beam-sensitive interfaces/interphases and material performance. Looking forward, numerous fresh understandings can be obtained through more advanced capabilities of cryo-EM, such as 3D tomography of SEI or operando biasing within TEM, which potentially generate a more comprehensive picture of SEI formation/distribution and dynamic changes within battery during operation. Coupled with AI-assisted data collection and processing, cryo-EM will continue bringing advancement of battery systems at a far faster rate.

In retrospect, the early development of cathode materials for battery and cryogenic functionality for electron microscopy occurred in the same era, but barely any interaction occurred for over four decades. Now electron microscopy finally made a detour back with cryogenic protection for advancing battery material characterizations. Unprecedented insights obtained from cryogenic techniques benefit not limited to the battery field, but to the whole material science community, stressing the importance of fully understanding material properties and behaviors over a vast temperature range. In this regard, exploring the phase diagram of complex materials at low temperature remains essential for better data interpretation from cryogenic techniques, which can yield new insights to the material study. With the advancement of high-end detectors and imaging techniques such as four-dimensional STEM, cryo-EM also gives chance to a more comprehensive picture of exotic physical properties of quantum materials and neuromorphic electronic materials when the motion of matters is slowed down at low temperature and can be then captured within a reasonable temporal scale.

ACKNOWLEDGMENTS

The authors gratefully acknowledge funding support from the U.S. Department of Energy, Office of Basic Energy Sciences, under Award Number DE-SC0002357. This work was also supported by the funding and collaboration agreement between

UC San Diego and Thermo Fisher Scientific on Advanced Characterization of Energy Materials. Y.S.M. is grateful for the funding support from Zable Endowed Chair for Energy Technologies at UC San Diego.

AUTHOR CONTRIBUTIONS

Conceptualization, D.C., M.Z., and Y.S.M.; Visualization, D.C., B.L., and G.R.; Writing – Original Draft, D.C.; Writing – Review and Editing, D.C., G.R., M.Z., and Y.S.M.; Supervision, M.Z. and Y.S.M.

DECLARATION OF INTERESTS

The authors declare no competing interests.

REFERENCES

1. Leblanc-Soreau, A., Danot, M., Trichet, L., and Rouxel, J. (1974). Les intercalaires Ax Ti S2 et Ax Zr S2. Structure et liaisons. (A = Li, Na, K, Rb, Cs). Mater. Res. Bull. *9*, 191–197.
2. Rao, G.V.S., and Tsang, J.C. (1974). Electrolysis method of intercalation of layered transition metal dichalcogenides. Mater. Res. Bull. *9*, 921–926.
3. Xu, K. (2014). Electrolytes and interphases in Li-ion batteries and beyond. Chem. Rev. *114*, 11503–11618.
4. Whittingham, M.S., and Fanwood, N.J. (1977). Chalcogenide Battery (Exxon Research and Engineering Company), pp. 1–5.
5. Goodenough, J.B., Mizushima, K., and Wiseman, P.J. (1976). Electrochemical Cell and Method of Making Ion Conductors for Said Cell, *13* (United Kingdom Atomic Energy Authority), pp. 258–283.
6. Thackeray, M., Johnson, P.J., de Picciotto, L.A., Bruce, P.G., and Goodenough, J.B. (1984). Electrochemical extraction of lithium from LiMn2O4. Mater. Res. Bull. *19*, 179–187.
7. Delmas, C., and Saadoune, I. (1992). Electrochemical and physical properties of the LixNi1−yCoyO2 phases. Solid State Ionics *56*, 370–375.
8. Padhi, A.K., Nanjundaswamy, K.S., and Goodenough, J.B. (1997). Phospho-olivines as positive-electrode materials for rechargeable lithium batteries. J. Electrochem. Soc. *144*, 1188.
9. Gao, Y., Myrtle, K., Zhang, M., Reimers, J.N., and Dahn, J.R. (1996). Valence band and its effects on the voltage profiles/Li electrochemical cells. Phys. Rev. B *54*, 16670–16675.
10. Wang, H., Jang, Y., Huang, B., Sadoway, D.R., and Chiang, Y. (1999). TEM study of electrochemical cycling-induced damage and disorder in LiCoO2 cathodes for rechargeable lithium batteries. J. Electrochem. Soc. *146*, 473–480.
11. Knoll, M., and Ruska, E. (1927). Beitrag zur geometrischen Elektronenoptik. I. Ann. Phys. *404*, 529–640.
12. Li, J.Y., Xu, Q., Li, G., Yin, Y.X., Wan, L.J., and Guo, Y.G. (2017). Research progress regarding Si-based anode materials towards practical application in high energy density Li-ion batteries. Mater. Chem. Front. *1*, 1691–1708.
13. Niu, C., Liu, D., Lochala, J.A., Anderson, C.S., Cao, X., Gross, M.E., Xu, W., Zhang, J.-G., Whittingham, M.S., Xiao, J., et al. (2021). Balancing interfacial reactions to achieve long cycle life in high-energy lithium metal batteries. Nat. Energy. https://doi.org/10.1038/s41560-021-00852-3.
14. Xu, W., Wang, J., Ding, F., Chen, X., Nasybulin, E., Zhang, Y., and Zhang, J.-G. (2014). Lithium metal anodes for rechargeable batteries. Energy Environ. Sci. *7*, 513–537.
15. Winter, M., Barnett, B., and Xu, K. (2018). Before Li ion batteries. Chem. Rev. *118*, 11433–11456.
16. Xu, K. (2004). Nonaqueous liquid electrolytes for lithium-based rechargeable batteries. Chem. Rev. *104*, 4303–4417.
17. Wang, X., Zhang, M., Alvarado, J., Wang, S., Sina, M., Lu, B., Bouwer, J., Xu, W., Xiao, J., Zhang, J.G., et al. (2017). New insights on the structure of electrochemically deposited lithium metal and its solid electrolyte interphases via cryogenic TEM. Nano Lett. *17*, 7606–7612.
18. Taylor, K.A., and Glaeser, R.M. (2016). Electron diffraction of frozen , hydrated protein crystals. Science *186*, 1036–1037.
19. Dubochet, J., Chang, J.J., Freeman, R., Lepault, J., and McDowall, A.W. (1982). Frozen aqueous suspensions. Ultramicroscopy *10*, 55–61.
20. Henderson, R., Baldwin, J.M., Ceska, T.A., Zemlin, F., Beckmann, E., and Downing, K.H. (1990). Model for the structure of bacteriorhodopsin based on high-resolution electron cryo-microscopy. J. Mol. Biol. *213*, 899–929.
21. Sigworth, F.J. (1998). A maximum-likelihood approach to single-particle image refinement. J. Struct. Biol. *122*, 328–339.
22. Shi, D., Nannenga, B.L., Iadanza, M.G., and Gonen, T. (2013). Three-dimensional electron crystallography of protein microcrystals. Elife *2*, 1–17.
23. Li, Y., Li, Y., Pei, A., Yan, K., Sun, Y., Wu, C.L., Joubert, L.M., Chin, R., Koh, A.L., Yu, Y., et al. (2017). Atomic structure of sensitive battery materials and interfaces revealed by cryo–electron microscopy. Science *358*, 506–510.
24. Lee, J.Z., Wynn, T.A., Alvarado, J., Schroeder, M.A., Wang, X., Guy-Bouyssou, D., Proust, M., and Meng, Y.S. (2019). Cryogenic focused ion beam characterization of lithium metal anodes. ACS Energy Lett. *4*, 489–493.
25. Zachman, M.J., Tu, Z., Choudhury, S., Archer, L.A., and Kourkoutis, L.F. (2018). Cryo-STEM mapping of solid–liquid interfaces and dendrites in lithium-metal batteries. Nature *560*, 345–349.
26. Jin, C., Liu, T., Sheng, O., Li, M., Liu, T., Yuan, Y., Nai, J., Ju, Z., Zhang, W., Liu, Y., et al. (2021). Rejuvenating dead lithium supply in lithium metal anodes by iodine redox. Nat. Energy, 26–28. https://doi.org/10.1038/s41560-021-00789-7.
27. Huang, W., Wang, H., Boyle, D.T., Li, Y., and Cui, Y. (2020). Resolving nanoscopic and mesoscopic heterogeneity of fluorinated species in battery solid-electrolyte interphases by cryogenic electron microscopy. ACS Energy Lett. *5*, 1128–1135.
28. Huang, W., Wang, J., Braun, M.R., Zhang, Z., Li, Y., Boyle, D.T., McIntyre, P.C., and Cui, Y. (2019). Dynamic structure and chemistry of the silicon solid-electrolyte interphase visualized by cryogenic electron microscopy. Matter *1*, 1232–1245.
29. Cheng, D., Wynn, T.A., Wang, X., Wang, S., Zhang, M., Shimizu, R., Bai, S., Nguyen, H., Fang, C., Kim, M., et al. (2020). Unveiling the stable nature of the solid electrolyte interphase between lithium metal and lipon via cryogenic electron microscopy. Joule. https://doi.org/10.2139/ssrn.3640837.
30. Yang, Y., Davies, D.M., Yin, Y., Borodin, O., Lee, J.Z., Fang, C., Olguin, M., Zhang, Y., Sablina, E.S., Wang, X., et al. (2019). High-efficiency lithium-metal anode enabled by liquefied gas electrolytes. Joule *3*, 1986–2000.
31. Doux, J.M., Yang, Y., Tan, D.H.S., Nguyen, H., Wu, E.A., Wang, X., Banerjee, A., and Meng, Y.S. (2020). Pressure effects on sulfide electrolytes for all solid-state batteries. J. Mater. Chem. A *8*, 5049–5055.
32. Aurbach, D. (1994). The surface chemistry of lithium electrodes in alkyl carbonate solutions. J. Electrochem. Soc. *141*, L1.

33. Peled, E. (1979). The electrochemical behavior of alkali and alkaline earth metals in nonaqueous battery systems—the solid electrolyte interphase model. J. Electrochem. Soc. *126*, 2047.

34. Wang, C., Meng, Y.S., and Xu, K. (2019). Fluorinating interphases. J. Electrochem. Soc. *166*, A5184–A5186.

35. Fang, C., Li, J., Zhang, M., Zhang, Y., Yang, F., Lee, J.Z., Lee, M.-H., Alvarado, J., Schroeder, M.A., Yang, Y., et al. (2019). Quantifying inactive lithium in lithium metal batteries. Nature *572*, 511–515.

36. Cao, X., Ren, X., Zou, L., Engelhard, M.H., Huang, W., Wang, H., Matthews, B.E., Lee, H., Niu, C., Arey, B.W., et al. (2019). Monolithic solid–electrolyte interphases formed in fluorinated orthoformate-based electrolytes minimize Li depletion and pulverization. Nat. Energy *4*, 796–805.

37. Shadike, Z., Lee, H., Borodin, O., Cao, X., Fan, X., Wang, X., Lin, R., Bak, S.M., Ghose, S., Xu, K., et al. (2021). Identification of LiH and nanocrystalline LiF in the solid–electrolyte interphase of lithium metal anodes. Nat. Nanotechnol. *16*, 549–554.

38. Han, B., Zhang, Z., Zou, Y., Xu, K., Xu, G., Wang, H., Meng, H., Deng, Y., Li, J., and Gu, M. (2021). Poor stability of Li2CO3 in the solid electrolyte interphase of a lithium-metal anode revealed by cryo-electron microscopy. Adv. Mater. *33*, 2100404.

39. Han, B., Li, X., Bai, S., Zou, Y., Lu, B., Zhang, M., Ma, X., Chang, Z., Meng, Y.S., and Gu, M. (2021). Conformal three-dimensional interphase of Li metal anode revealed by low-dose cryoelectron microscopy. Matter *4*, 3741–3752.

40. Han, B., Zou, Y., Zhang, Z., Yang, X., Shi, X., Meng, H., Wang, H., Xu, K., Deng, Y., and Gu, M. (2021). Probing the Na metal solid electrolyte interphase via cryo-transmission electron microscopy. Nat. Commun. *12*, 1–8.

41. Wang, X., Pawar, G., Li, Y., Ren, X., Zhang, M., Lu, B., Banerjee, A., Liu, P., Dufek, E.J., Zhang, J.G., et al. (2020). Glassy Li metal anode for high-performance rechargeable Li batteries. Nat. Mater. *19*, 1339–1345.

42. Yuan, H., Nai, J., Tian, H., Ju, Z., Zhang, W., Liu, Y., Tao, X., and Lou, X.W. (2020). An ultrastable lithium metal anode enabled by designed metal fluoride spansules. Sci. Adv. *6*, 1–10.

43. Yuan, H., Nai, J., Fang, Y., Lu, G., Tao, X., and Lou, X.W. (2020). Double-shelled C@MoS2 structures preloaded with sulfur: an additive reservoir for stable lithium metal anodes. Angew. Chem. Int. Ed. *59*, 15839–15843.

44. Fang, C., Lu, B., Pawar, G., Zhang, M., Cheng, D., Chen, S., Ceja, M., Doux, J.-M., Musrock, H., Cai, M., et al. (2021). Pressure-tailored lithium deposition and dissolution in lithium metal batteries. Nat. Energy *6*, 987–994.

45. Han, B., Zou, Y., Xu, G., Hu, S., Kang, Y., Qian, Y., Wu, J., Ma, X., Yao, J., Li, T., et al. (2021). Additive stabilization of SEI on graphite observed using cryo-electron microscopy. Energy Environ. Sci. https://doi.org/10.1039/D1EE01678D.

46. He, Y., Jiang, L., Chen, T., Xu, Y., Jia, H., Yi, R., Xue, D., Song, M., Genc, A., Bouchet-Marquis, C., et al. (2021). Progressive growth of the solid–electrolyte interphase towards the Si anode interior causes capacity fading. Nat. Nanotechnol. https://doi.org/10.1038/s41565-021-00947-8.

47. Alvarado, J., Schroeder, M.A., Zhang, M., Borodin, O., Gobrogge, E., Olguin, M., Ding, M.S., Gobet, M., Greenbaum, S., Meng, Y.S., et al. (2018). A carbonate-free, sulfone-based electrolyte for high-voltage Li-ion batteries. Mater. Today *21*, 341–353.

48. Yang, Y., Yin, Y., Davies, D.M., Zhang, M., Mayer, M., Zhang, Y., Sablina, E.S., Wang, S., Lee, J.Z., Borodin, O., et al. (2020). Liquefied gas electrolytes for wide-temperature lithium metal batteries. Energy Environ. Sci. *13*, 2209–2219.

49. Zhang, Z., Yang, J., Huang, W., Wang, H., Zhou, W., Li, Y., Li, Y., Xu, J., Huang, W., Chiu, W., et al. (2021). Cathode-electrolyte interphase in lithium batteries revealed by cryogenic electron microscopy. Matter *4*, 302–312.

50. Xing, X., Li, Y., Wang, X., Petrova, V., Liu, H., and Liu, P. (2019). Cathode electrolyte interface enabling stable Li–S batteries. Energy Storage Mater. *21*, 474–480.

51. Ma, C., Cheng, Y., Yin, K., Luo, J., Sharafi, A., Sakamoto, J., Li, J., More, K.L., Dudney, N.J., and Chi, M. (2016). Interfacial stability of Li metal-solid electrolyte elucidated via in situ electron microscopy. Nano Lett. *16*, 7030–7036.

52. Liu, X., Chen, Y., Hood, Z.D., Ma, C., Yu, S., Sharafi, A., Wang, H., An, K., Sakamoto, J., Siegel, D.J., et al. (2019). Elucidating the mobility of H+ and Li+ ions in (Li6.25-:XHxAl0.25)La3Zr2O12 via correlative neutron and electron spectroscopy. Energy Environ. Sci. *12*, 945–951.

53. Cheng, M., Rangasamy, E., Liang, C., Sakamoto, J., More, K.L., and Chi, M. (2015). Excellent stability of a lithium-ion-conducting solid electrolyte upon reversible LI+/H+ exchange in aqueous solutions. Angew. Chem. Int. Ed. *54*, 129–133.

54. Liu, X., Garcia-Mendez, R., Lupini, A.R., Cheng, Y., Hood, Z.D., Han, F., Sharafi, A., Idrobo, J.C., Dudney, N.J., Wang, C., et al. (2021). Local electronic structure variation resulting in Li 'filament' formation within solid electrolytes. Nat. Mater. *20*, 1485–1490.

55. Sheng, O., Zheng, J., Ju, Z., Jin, C., Wang, Y., Chen, M., Nai, J., Liu, T., Zhang, W., Liu, Y., et al. (2020). In situ construction of a LiF-enriched interface for stable All-solid-state batteries and its origin revealed by cryo-TEM. Adv. Mater. *32*, 1–10.

56. Egerton, R.F., Li, P., and Malac, M. (2004). Radiation damage in the TEM and SEM. Micron *35*, 399–409.

57. Jiang, N. (2015). Electron beam damage in oxides: a review. Rep. Prog. Phys. *79*, 016501.

58. Wang, X., Li, Y., and Meng, Y.S. (2018). Cryogenic electron microscopy for characterizing and diagnosing batteries. Joule *2*, 2225–2234.

59. Schorb, M., Haberbosch, I., Hagen, W.J.H., Schwab, Y., and Mastronarde, D.N. (2019). Software tools for automated transmission electron microscopy. Nat. Methods *16*, 471–477.

60. Wang, F., Graetz, J., Moreno, M.S., Ma, C., Wu, L., Volkov, V., and Zhu, Y. (2011). Chemical distribution and bonding of lithium in intercalated graphite: identification with optimized electron energy loss spectroscopy. ACS Nano *5*, 1190–1197.

61. Güven, G., and Oktay, A.B. (2018). Nanoparticle detection from TEM images with deep learning. In 26th IEEE Signal Processing and Communications Applications Conference SIU 2018, pp. 1–4. https://doi.org/10.1109/SIU.2018.8404468.

62. Horwath, J.P., Zakharov, D.N., Mégret, R., and Stach, E.A. (2020). Understanding important features of deep learning models for segmentation of high-resolution transmission electron microscopy images. Npj Comput. Mater. *6*, 1–9.

63. Ronneberger, O., Fischer, P., and Brox, T. (2015). INet: convolutional networks for biomedical image segmentation. arXiv, 1–8. https://doi.org/10.1109/ACCESS.2021.3053408.

64. Hill, J., Mulholland, G., Persson, K., Seshadri, R., Wolverton, C., and Meredig, B. (2016). Materials science with large-scale data and informatics: unlocking new opportunities. MRS Bull. *41*, 399–409.

65. Heron, M., Hanson, V.L., and Ricketts, I. (2013). Open source - accessibility and limitations. J. Interact. Sci. *1*, 1–10.

66. Rafique, K., Tareen, A.W., Saeed, M., Wu, J., and Qureshi, S.S. (2011). Cloud computing economics opportunities and challenges. In Proceedings - 2011 4th IEEE International Conference on Broadband Network and Multimedia Technology, IC-BNMT 2011 (IEEE), pp. 401–406. https://doi.org/10.1109/ICBNMT.2011.6155965.

67. Cusumano, M. (2010). Cloud computing and SaaS as new computing platforms. Commun. ACM *53*, 27–29.